Precision Engineering 35 (2011) 686–692

Contents lists available at ScienceDirect

Precision Engineering

journal homepage: www.elsevier.com/locate/precision

# Multi-probe scanning system comprising three laser interferometers and one autocollimator for measuring flat bar mirror profile with nanometer accuracy

Ping Yang[a], Tomohiko Takamura[a], Satoru Takahashi[a], Kiyoshi Takamasu[a,*], Osamu Sato[b], Sonko Osawa[b], Toshiyuki Takatsuji[b]

[a] Department of Precision Engineering, The University of Tokyo, Hongo 7-3-1, Bunkyo-ku, Tokyo 113-8656, Japan
[b] National Metrology Institute of Japan, National Institute of Advanced Industrial Science and Technology, Umezono1-1-1, Tsukuba, Ibaraki 305-8563, Japan

ARTICLE INFO

*Article history:*
Received 4 January 2011
Received in revised form 20 April 2011
Accepted 10 May 2011
Available online 27 May 2011

*Keywords:*
Multi-probe method
Laser interferometers
Autocollimator
Profile
Motion errors

ABSTRACT

This paper describes a multi-probe scanning system comprising three laser interferometers and one autocollimator to measure a flat bar mirror profile with nanometer accuracy. The laser interferometers probe the surface of the flat bar mirror that is fixed on top of a scanning stage, while the autocollimator simultaneously measures the yaw error of the scanning stage. The flat bar mirror profile and horizontal straightness motion error are reconstructed by an application of simultaneous linear equations and least-squares method. Measurement uncertainties of the flat bar mirror profile were numerically evaluated for different installation distances between the laser interferometers. The average measurement uncertainty was found to be only 10 nm with installation distances of 10 and 21 mm between the first and second, and first and third interferometers, respectively. To validate the simulation results, a prototype system was built using an X–Y linear stage driven by a stepper motor with steps of 1 mm along the X direction. Experiments were conducted with fixed interferometers distances of 10 and 21 mm, as in the simulation, on a flat bar mirror with a profile known to an accuracy of $\lambda = 632.8$ nm. The average value of two standard deviations (95%) of the profile calculated over ten experiments was approximately 10 nm. Other results from the experiment showed that the system can also measure the yaw and horizontal straightness motion errors successfully at a high horizontal resolution. Comparing with the results measured by ZYGO's interferometer, our measured data excluding some edge points showed agreement to within approximately 10 nm. Therefore, we concluded that our measurement profile has an accuracy in the nanometer range.



## 1. Introduction

With the development of super-precision machining technology, accuracies of large-scale parts such as optical components, silicon wafers, and liquid crystal panels are already on the order of nanometers. It has also become increasingly important to evaluate surface geometry (straightness, flatness) with nanometer accuracy.

Scanning systems with optical components have been widely used in the field of engineering metrology to meet these requirements [1–4]. However, these scanning systems generally suffer from positional and angular errors of the scanning stage prompting the need for measurement and calibration of the relative motion errors. Currently, a laser interferometer system with a specialized reflector is the typical instrument for measuring translational and angular errors [5]. Moreover, a high accuracy autocollimator has been developed and widely used for measuring rotational errors and surface profiles [6,7]. These two components are considered to be the most reliable and accurate parametric calibration instruments. Thus, a multi-probe scanning system that employs three laser interferometers and one autocollimator has been developed to measure a flat bar mirror profile with nanometer accuracy, while multiple motion errors are measured simultaneously.

The principle of the multi-probe scanning method is based on an error separation technique originally proposed by Whitehouse in 1976 [8] and widely used in the precision measurement field [9,10]. Multi-probe methods for measuring straightness and roundness have been extensively developed. These methods began with research into sequential two-point and three-point methods [1,11] that not only measure the straightness motion error of the guideway, but also the straightness of the objective surface. However, these methods are limited in terms of horizontal resolution, and the results are affected by systematic and random errors of the output sensors. In order to improve the horizontal resolution, integration multi-probe methods have been proposed [12]. However, in the application of the integration multi-probe method it is still difficult to compensate for the systematic errors of the probes for zero deviation [13,14]. A spatial frequency method using a data processing method by discrete Fourier transform (DFT) is considered to be a

* Corresponding author. Tel.: +81 3 5841 6450; fax: +81 3 5841 8554.
*E-mail address:* takamasu@pe.t.u-tokyo.ac.jp (K. Takamasu).

0141-6359/$ – see front matter © 2011 Elsevier Inc. All rights reserved.
doi:10.1016/j.precisioneng.2011.05.001

modification of the three-point roundness measurement method [15]. The spatial frequency domain two-point method which combines two data sets from two-point methods with different sensor distances has been proposed by Elster [16,17]. The calibration of systematic errors for this method has also been discussed [18]. In addition, multi-probe methods utilizing more than three displacement sensors and using different software algorithms have been proposed [2,19,20]. Other compensation methods such as adding one autocollimator or a reversal operation have been developed to improve the multi-probe method [21].

In this paper, we begin by setting up simultaneous linear equations that express the linear relationship between the measured parameters and the unknowns. We then analyze the measurement uncertainty for the flat bar mirror profile and calculate the unknown parameters by applying the least-squares method [22–26]. The random and systematic errors of the probes are considered and the measurement uncertainty is calculated by the simulation. Comparing with the experiment results, the multi-probe scanning method can precisely reach nanometer scale measurement.

## 2. Measurement principle

### 2.1. Principle of multi-probe scanning method

In the multi-probe scanning system, the laser interferometers probe the surface of a flat bar mirror that is fixed on top of an X–Y scanning stage, while the autocollimator simultaneously measures the yaw error of the scanning stage [22]. Unlike the case where the displacement sensors are fixed on a moving scanner, the laser interferometers are mounted on stationary housings, as shown in Fig. 1. During the measurement, the scanning stage moves in steps. And at each step, a computer automatically collects the data from the laser interferometers and the autocollimator. Let the corresponding laser interferometers and autocollimator outputs be $m_1(n), m_2(n), m_3(n)$, and $m_a(n)$, respectively, then they can be expressed as follows:

$$\begin{cases} m_1(n) = f(x_n+0) + e_s(n) + 0\cdot e_y(n) + u_1 + b_0 \\ m_2(n) = f(x_n+D_1) + e_s(n) + D_1\cdot e_y(n) + u_2 + b_0 \\ m_3(n) = f(x_n+D_2) + e_s(n) + D_2\cdot e_y(n) + u_3 + b_0 \\ m_a(n) = e_y(n) + u_a \end{cases}, \quad n = 1 \ldots N_s \,. \tag{1}$$

Here $f(x_n)$ denotes the flat bar mirror profile; $e_y(n)$ and $e_s(n)$ denote the yaw and horizontal straightness motion errors of the moving stage, respectively at each step $n$; $D_1$ is the installation distance between the 1st and 2nd laser interferometers; $D_2$ is the installation distance between the 1st and 3rd laser interferometers; $u_1, u_2, u_3$ and $u_a$ are the offsets of each probe; and $b_0$ is an unknown parameter in the measurement. The number of sampling points of the flat bar mirror profile is $N$ and the number of sampling points of the motion errors is given by $N_s = N - d_2$. The parameter $d_2$ is defined as $d_2 = D_2/s$ that is the normalized distance of the 3rd laser interferometer. The measuring step distance of the scanning stage is $s$ and $L = n \times s$ specifies the moving scale of the stage, as shown in Fig. 1. For the analysis here, the step distance $s$ is determined by the number of the laser interferometers and their relative distances. We discuss how to select the value of $s$ in Section 2.2.

### 2.2. Data processing

#### 2.2.1. Simultaneous linear equations

In order to eliminate the unknown parameters from Eq. (1), we define the supplementary function Eq. (2).

$$\begin{cases} e_1(n) = e_s(n) + u_1 + b_0 \\ e_2(n) = e_y(n) + u_a \\ c_j = u_j - u_1 - D_j\cdot u_a, \ \ j = 2, 3 \end{cases}, \quad n = 1 \ldots N_s \,. \tag{2}$$

Here $e_1(n)$ and $e_2(n)$ denote horizontal straightness motion $e_s(n)$ and yaw errors $e_y(n)$ with systematic and random errors at each step, respectively. Then, substituting Eq. (2) into (1), the measurement equations can be simplified as follows:

$$\begin{cases} m_1(n) = f(x_n) + e_1(n) \\ m_2(n) = f(x_n+D_1) + e_1(n) + D_1\cdot e_2(n) + c_2 \\ m_3(n) = f(x_n+D_2) + e_1(n) + D_2\cdot e_2(n) + c_3 \\ m_a(n) = e_2(n) \end{cases}, \quad n = 1 \ldots N_s \,. \tag{3}$$

According to the linear relationship between the measured data and the objective parameters, the whole measurement process can be expressed simply as a set of simultaneous linear equations,

$$\mathbf{Y} = \mathbf{AX}, \tag{4}$$

where $\mathbf{Y}$ denotes the measured vectors

$$\mathbf{Y} = [m_1(1), \cdots, m_1(N_s), \cdots, m_3(1), \cdots, m_3(N_s), m_a(1), \cdots, m_a(N_s)]^T. \tag{5}$$

and $\mathbf{A}$ is the Jacobian matrix constructed by the differential of $\mathbf{Y}$ and $\mathbf{X}$. The unknown vectors $\mathbf{X}$ are the flat bar mirror profile and the motion errors.

$$\mathbf{X} = [f(x_1), \cdots, f(x_{N-2}), e_1(1), \cdots, e_1(N_s), e_2(1), \cdots, e_2(N_s), c_2, c_3]^T. \tag{6}$$

From Eq. (6), only $N-2$ components of the flat bar mirror profile can be varied independently. The best straight-line fit of the resulting profile $f(x_n)$ is used to calculate the last two points of the profile. Each point of the profile can be changed by any straight line when $e_1(n)$ and $e_2(n)$ are correspondingly changed at the same time.

$$\sum_{n=1}^{N} x_n f(x_n) = \sum_{n=1}^{N} f(x_n) = 0. \tag{7}$$

The constraints of Eq. (7) can, for instance, be considered explicitly by substituting $f(x_{N-1})$ and $f(x_N)$ as follows:

$$\begin{cases} f(x_{N-1}) = \displaystyle\sum_{n=1}^{N-2} (n-N) f(x_n), \\ f(x_N) = \displaystyle\sum_{n=1}^{N-2} (N-1-n) f(x_n). \end{cases} \tag{8}$$

For a solution of the matrix $\mathbf{X}$ to exist according to Eq. (4), two additional conditions must be satisfied.

1. The row number $\mathbf{A}$ ($P$) must be greater than or to equal the column number $\mathbf{A}$ ($Q$). ($P \geqq Q$).
2. The rank of $\mathbf{A}$ must be equal to the column number $\mathbf{A}$ ($Q$).

For condition 1 to be satisfied, $P$ and $Q$ are calculated as follows:

$$\begin{aligned} &P = N_s \times (3+1) = 4N_s, \\ &Q = N - 2 + 2\cdot N_s + 3 - 1 = 3N_s + d_2, \\ &P \geq Q \Rightarrow N_s \geq d_2. \end{aligned} \tag{9}$$

Eq. (9) then sets $N_s \geq D_2/s$, which means that the number of sampling points of the motion errors is greater than or equal to the normalized distance of the 3rd laser interferometer. The least-squares solution exists when this condition is met.

For condition 2, the rank of $\mathbf{A}$ is determined by the normalized distances of the laser interferometers ($d_1$, $d_2$). Therefore, the greatest common divisor (GCD) of $d_1$ and $d_2$ should be 1. (GCD ($d_1$, $d_2$) = 1).

The parameters $D_1$, $D_2$, and $s$ are chosen to satisfy these conditions.

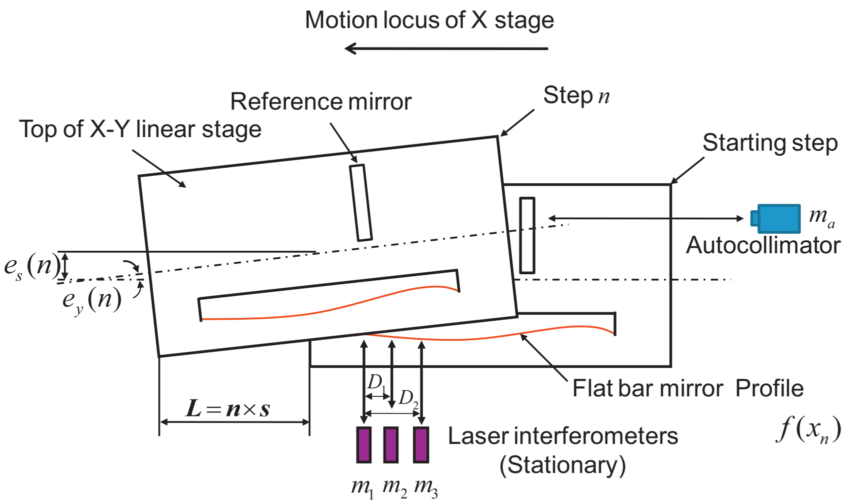


**Fig. 1.** Principle of multi-probe scanning method.

### 2.2.2. Least-squares method

From Eq. (4), the measured model **Y** comprises a linear combination of the objective parameters **X**. In the measurement system, **Y** is assumed to have random errors. The sources of error for each measured vector, which follow the normal distribution, are dependent. Accordingly, the error matrix **S** that denotes the error variance between each measurement point is given by

$$\mathbf{S} = \begin{pmatrix} \sigma_1^2 & & & & & & & & & \\ & \ddots & & & & & & & 0 & \\ & & \sigma_1^2 & & & & & & & \\ & & & \ddots & & & & & & \\ & & & & \sigma_3^2 & & & & & \\ & & & & & \ddots & & & & \\ & & & & & & \sigma_3^2 & & & \\ & & & & & & & \sigma_a^2 & & \\ & 0 & & & & & & & \ddots & \\ & & & & & & & & & \sigma_a^2 \end{pmatrix}. \quad (10)$$

Here $\sigma_1$ denotes the standard deviation of the 1st laser interferometer, $\sigma_3$ is the standard deviation of the 3rd laser interferometer, and $\sigma_a$ is the standard deviation of the autocollimator.

Utilizing the linear least-squares method to calculate the objective matrix **X**, we obtain:

$$\mathbf{X} = \left(\mathbf{A}^t\mathbf{S}^{-1}\mathbf{A}\right)^{-1}\mathbf{A}^t\mathbf{S}^{-1}\mathbf{Y}. \quad (11)$$

### 2.3. Reconstruction of uncertainty

From the reconstruction procedure, the measurement uncertainty associated with the reconstructed flat bar mirror profile can be derived. The reliability of the reconstructed data and its associated measurement uncertainty can be assessed via a criterion. The associated uncertainty of the measurement process is calculated via the error propagation matrix $\mathbf{S_X}$ that is deformed in the least-squares method, as shown in Eq. (12). The vectors on the diagonal of $\mathbf{S_X}$ are the square values of the measurement uncertainties of the flat bar mirror profile $\sigma(n)$ from 1 to $N-2$.

$$\mathbf{S_X} = (\mathbf{A^T}\mathbf{S}^{-1}\mathbf{A})^{-1} = \begin{pmatrix} r_{11} & \cdots & r_{1n} \\ \vdots & \ddots & \vdots \\ r_{n1} & \cdots & r_{nn} \end{pmatrix}, \quad (n = 1, \cdots, N-2), \quad (12)$$

$$\sigma(n) = \sqrt{r_{nn}}, \quad (n = 1, \ldots, N-2), \quad (13)$$

$$\begin{cases} \sigma(N-1) = \sqrt{\sum_{i=1}^{N-2}\sum_{j=1}^{N-2}(i-N)(j-N)S_X(i,j)}, \\ \sigma(N) = \sqrt{\sum_{i=1}^{N-2}\sum_{j=1}^{N-2}(N-1-i)(N-1-j)S_X(i,j)}, \end{cases} \quad (14)$$

$$\sigma = \sigma(n), \quad (n = 1, \ldots, N). \quad (15)$$

Eq. (13) denotes the measurement uncertainty of sampling points from 1 to $N-2$, and $\sigma(N-1)$ and $\sigma(N)$ denote the uncertainty of the last two points, respectively. From Eqs. (12) and (14), we can note the uncertainties associated with $N$ and $\sigma_x$. Thus, the measurement uncertainty values in every measurement points are obtained from Eq. (15).

## 3. Uncertainty simulation

The multi-probe scanning method was evaluated theoretically by computer simulation. From Eq. (3), we set up three laser interferometers and one autocollimator in the simulation model. For the simulation, $f(x_n)$ is predefined in a profile curve; $e_1(n)$ and $e_2(n)$ are random numbers from the initialization; $L$ is set to 100 mm. According to the GCD condition, we choose different sets of $D_1$ and $D_2$ values, with $s$ set to 1 mm, as shown as Table 1, in order to analyze the factors influencing the measurement uncertainty of the flat bar mirror profile. Then, each measured data can be substituted by the parameters mentioned above. The standard deviation of the laser interferometers and autocollimator were set to $\sigma_1 = \sigma_2 = \sigma_3 = 3.5$ nm and $\sigma_a = 0.23$ μrad. These values were taken

**Table 1**
Different installation distances of laser interferometers.

| Group | $D_1$ (mm) | $D_2$ (mm) |
|---|---|---|
| No. 1 | 2 | 5 |
| No. 2 | 4 | 9 |
| No. 3 | 5 | 11 |
| No. 4 | 10 | 21 |
| No. 5 | 15 | 31 |

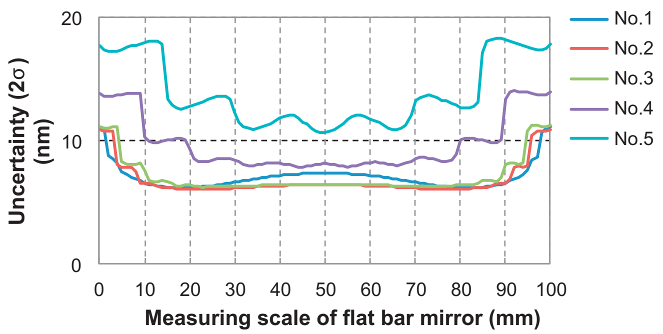


**Fig. 2.** Relationship between different installation distances of laser interferometers and measurement uncertainty of flat bar mirror profile for $\sigma_1 = \sigma_2 = \sigma_3 = 3.5$ nm and $\sigma_a = 0.23$ µrad.

from the model specifications (laser interferometers: 10705A, Agilent; autocollimator: Elcomat 3000, Moller-Wedel Optical). From Eq. (11), we can calculate the objective profile by the simulation.

The measurement uncertainty of objective profile can be derived from the reconstruction procedure as shown in Eq. (11). Thus, we can numerically simulate the measurement uncertainty of flat bar mirror $\sigma$ from Eqs. (12) and (14), and the simulation results of $2\sigma$ are shown in Fig. 2 with different installation distances of laser interferometers.

Fig. 3 shows the relationship between different sets of installation distances of laser interferometers and the average values of uncertainty from the results in Fig. 2. From Fig. 3, the average uncertainty values increase almost continuously with increasing installation distance ($D_1$, $D_2$). Thus, the smaller the installation distances, the higher the accuracy. However, it is difficult to arrange the installation distances to be less than 6 mm because the diameter of the laser beam is 6 mm. As a result, we chose group No. 4 ($D_1$ = 10 mm, $D_2$ = 21 mm) for our experiment. The average measurement uncertainty is approximately 10 nm, which is acceptable for nanometer scale measurements.

## 4. Experiment

### 4.1. Experimental setup

The experiment is designed to measure the flat bar mirror profile with nanometer accuracy and was performed by three laser interferometers and one autocollimator operating simultaneously. Fig. 4 shows a block diagram of the experiment, which is composed of a flat bar mirror, an XY stepper motor stage, laser interferometers, receivers, beam splitters, optical refection mirrors, and an autocollimator. In the experiment, the laser interferometers probed the surface of the flat bar mirror which is fixed on top of the scanning stage, while the autocollimator simultaneously measured the yaw error of the scanning stage by the reference mirror 6 (Fig. 4). The scanning direction along the X-axis was performed from right to left as shown in Fig. 4. A feature of this optical design is that we can adjust the installation distances of interferometer by moving the corresponding mirror (mirrors 3, 4, and 5). The laser interferometers are denoted LI1, LI2, and LI3, respectively, in Fig. 4.

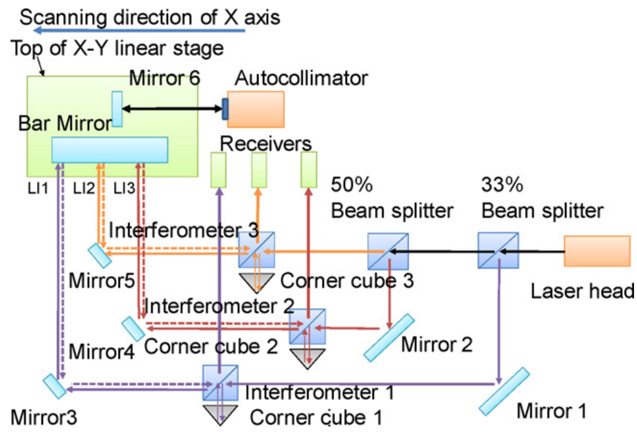


**Fig. 4.** Block diagram of experimental setup.

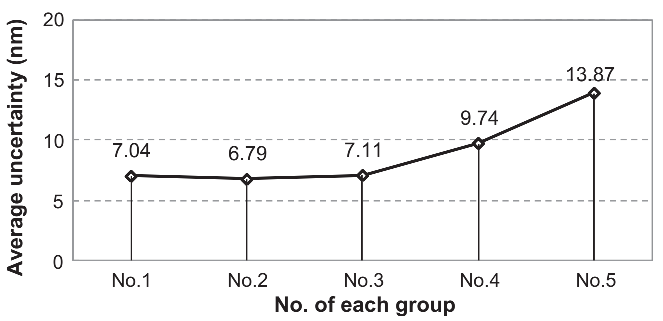


**Fig. 3.** Relationship between different installation distances of laser interferometers and average measurement uncertainty of flat bar mirror profile for $\sigma_1 = \sigma_2 = \sigma_3 = 3.5$ nm and $\sigma_a = 0.23$ µrad.

In the equipment setup, the sampling length of the flat bar mirror is 100 mm because the valid size of the flat bar mirror is approximately 100 mm × 30 mm with an accuracy of $\lambda = 632.8$ nm. The actual experimental setup is shown in Fig. 5. Setting $D_1 = 10$ mm, $D_2 = 21$ mm, and $s = 1$ mm, and for $N = 100$, gives $N_s = N - d_2$ as 79.

### 4.2. Stability of each sensor

The accuracies of the laser interferometers are sensitive to the measurement environment and other external factors. Therefore, we measured the stability of each sensor at the first sampling point before performing the experiment. The stability results of the laser interferometers and the autocollimator are shown in Figs. 6 and 7, respectively. The measuring time was 5 min and this is approximately the same duration as a whole measurement process. The standard deviations of the laser interferometers and the autocollimator were calculated to be $\sigma_1 = \sigma_2 = \sigma_3 = 3.5$ nm, and $\sigma_a = 0.23$ µrad.

### 4.3. Experiment results

The yaw errors along the X-axis $e_2(n)$ from ten repetitions of the experiments are presented in Fig. 8. The range of $e_2(n)$ is approx-

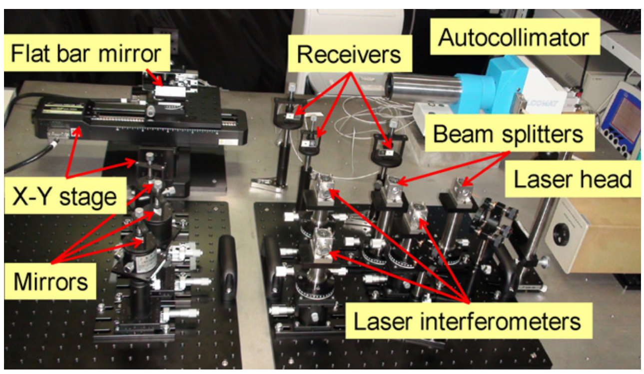


**Fig. 5.** Actual experimental setup.

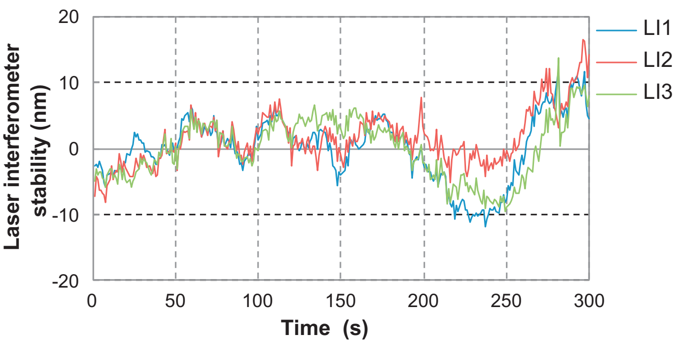


**Fig. 6.** Laser interferometer stability.

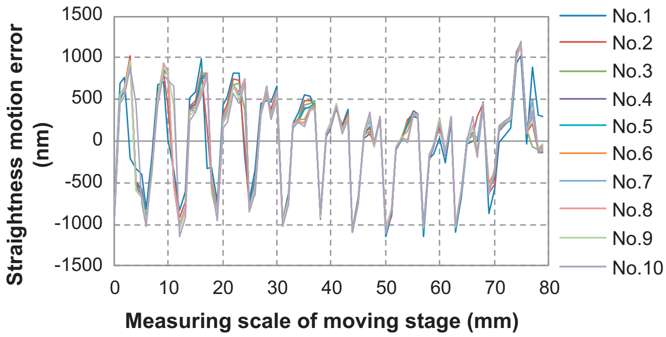


**Fig. 9.** Straightness motion error of X stage.

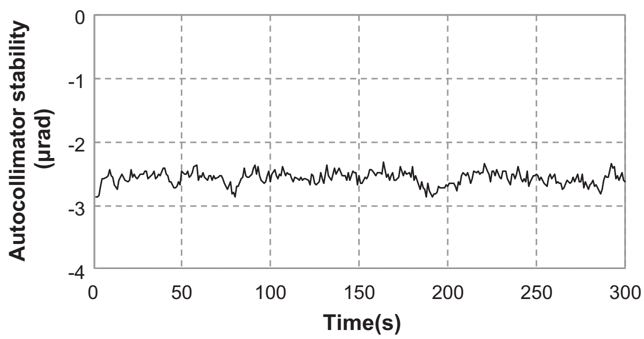


**Fig. 7.** Autocollimator stability.

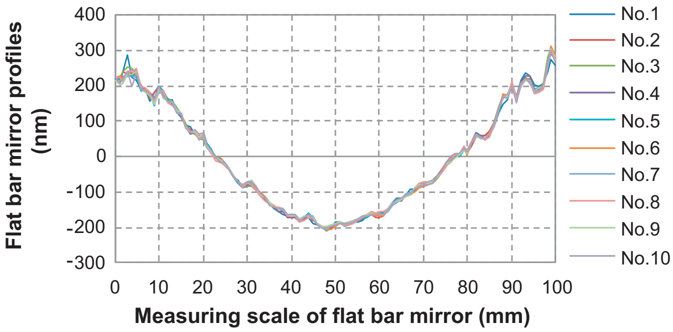


**Fig. 10.** Profile of flat bar mirror.

imately 40 μrad. The horizontal straightness motion errors along the *X*-axis $e_1(n)$, obtained by applying the simultaneous equation and least-squares method, are shown in Fig. 9. The range of $e_1(n)$ is approximately 2 μm. The reconstructed profiles of the flat bar mirror $f(x_n)$ are shown in Fig. 10, and the profiles are reproduced well for each of the ten measurements.

The two standard deviations (95%) values of the flat bar mirror profile calculated over the ten experiments are shown in Fig. 11 indicated by the red curve; the average value is approximately 10 nm. According to Fig. 2, the simulated measurement uncertainty ($2\sigma$) is shown in Fig. 11 and indicated by the black curve with parameters set as per group No. 4. Comparing these two curves, we conclude that the two standard deviations of the flat bar mirror profile is mainly fitting the range of $2\sigma$. The multi-probe scanning method performs well with a small deviation of 10 nm in the measurement of the flat bar mirror profile, and measures the horizontal straightness motion and yaw errors successfully with a high horizontal resolution. Moreover, in the comparison between the simulated measurement uncertainty ($\pm 2\sigma$) and the difference curves between the average value of ten profiles and each profile (Fig. 12), we note that the difference curves mainly lie with $\pm$10 nm ($\pm 2\sigma$) verifying nanometer accuracy.

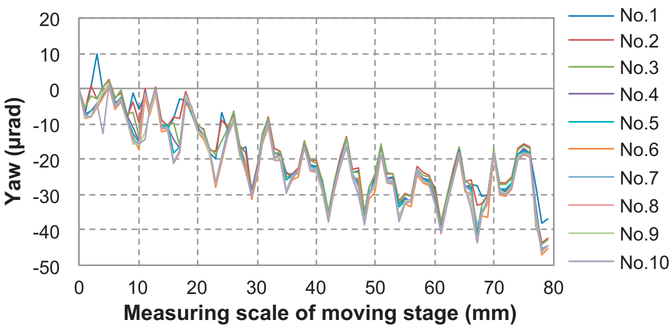


**Fig. 8.** Yaw error of X stage.

### 4.4. Comparison with ZYGO's interferometer system

To confirm the measurement accuracy of the flat bar mirror profile, we compared our profile data with results measured by ZYGO's interferometer system. The average flat bar mirror profile for ten experiments is indicated in Fig. 13 by the red curve. The profile measured by the ZYGO's interferometer system is indicated by the black curve. The comparison shows that the two profiles are approximately the same within the deviation range of 10 nm, excluding some points at the edge of the mirror. This is a limitation of the multi-probe scanning method

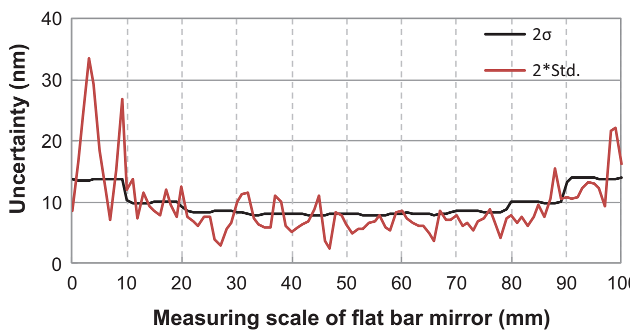


**Fig. 11.** Comparison of two standard deviations of ten times flat bar mirror profiles (red line) with simulated measurement uncertainty (black line) ($2\sigma$). (For interpretation of the references to color in this figure legend, the reader is referred to the web version of the article.)

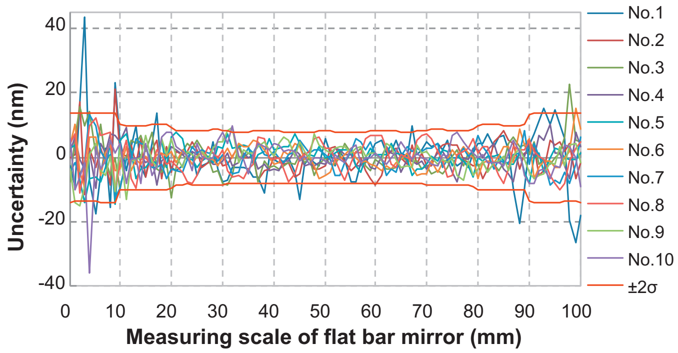


**Fig. 12.** Comparison of simulated measurement uncertainty ($\pm 2\sigma$) of flat bar mirror profile with difference between average value of ten profiles and each profile.

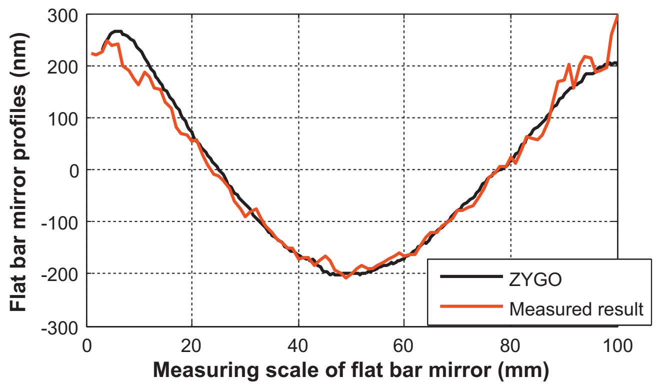


**Fig. 13.** Comparison of average flat bar mirror profile with profile measured by ZYGO's interferometer system.

because these points can only be measured by a single displacement sensor.

## 5. Conclusions and future works

We have devised a multi-probe scanning method using three laser interferometers and one autocollimator to measure a flat bar mirror profile with nanometer accuracy. In the measurement system, the flat bar mirror profile is reconstructed by the application of simultaneous linear equations and least-squares method, and the yaw and horizontal straightness motion errors of the scanning stage can be measured. From the simulation and experiment results, we can make the following conclusions.

The simulation results indicate that the average measurement uncertainty of the flat bar mirror profile increases almost continuously with increasing installation distances between the laser interferometers ($D_1$, $D_2$). When we set $D_1 = 10$ mm, $D_2 = 21$ mm, $s = 1$ mm, $\sigma_1 = \sigma_2 = \sigma_3 = 3.5$ nm, and $\sigma_a = 0.23$ μrad, the average measurement uncertainty is approximately 10 nm.

From Section 2.3, we found that the standard deviation of each sensor is essential to the measurement uncertainty. Thus, we measured the stability of each sensor at the starting point in the real environment before performing the experiment. The standard deviations of the laser interferometers are the same $\sigma_1 = \sigma_2 = \sigma_3 = 3.5$ nm, and standard deviation of the autocollimator was calculated as $\sigma_a = 0.23$ μrad and these were defined as the actual parameters for the experiment.

From the experiment, the two standard deviations of the flat bar mirror profile is mainly fitting the simulated measurement uncertainty of 10 nm ($2\sigma$). Moreover, the difference curves between the average value of ten profiles and each profile mainly lie within the simulated measurement uncertainty of $\pm 10$ nm ($\pm 2\sigma$). In addition, the multi-probe scanning system can also measure the yaw and horizontal straightness motion errors successfully with a high horizontal resolution.

Comparing with the results measured by ZYGO's interferometer, our measured data excluding some edge points showed agreement to within approximately 10 nm. Therefore, we concluded that our measurement profile has an accuracy in the nanometer range. However, there are some variations in the flat bar mirror profile of our measurement results. They are due to some additional error sources in the measurement process, such as the accuracy of moving the scanning stage and the misalignment of the optical devices. These error sources will be analyzed in greater detail in the future.

## Acknowledgements

Ping Yang wishes to thank the supports from the Japanese Government (Monbukagakusho: MEXT) Scholarship and Japanese Global COE Program, "Global Center of Excellence for Mechanical Systems Innovation".

## References

[1] Makosch G, Drollinger B. Surface profile measurement with a scanning differential ac interferometer. Appl Opt 1984;23–24:4544–53.
[2] Weingärtner I, Elster C. System of four distance sensors for high accuracy measurement of topography. Prec Eng 2004;28:164–70.
[3] Elster C, Weingärtner I, Schulz M. Coupled distance sensor systems for high-accuracy topography measurement: accounting for scanning stage and systematic sensor errors. Prec Eng 2006;30:32–8.
[4] Gao W, Yokoyama J, Kojima H, Kiyono S. Precision measurement of cylinder straightness using a scanning multi-probe system. Prec Eng 2002;26:279–88.
[5] Gao W, Arai Y, Shibuya A, Kiyono S, Park CH. Measurement of multi-degree-of-freedom error motions of a precision linear air-bearing stage. Prec Eng 2006;30:96–103.
[6] Gerhardt J, Geckeler RD, Schulz M, Elster C. High-accuracy profile form measurement by a scanning system consisting of an angle sensor and coupled distance sensors. Proc SPIE 2005;5856:385–92.
[7] Geckeler RD, Just A. Distance-dependent influences on angle metrology with autocollimators in deflectometry. Proc SPIE 2008;7077:70770B.
[8] Whitehouse DJ. Some theoretical aspects of error separation techniques in surface metrology. J Phys E: Sci Instrum 1976;9:531–6.
[9] Evans CJ, Hocken RJ, Estler WT. Self-calibration: reversal, redundancy, error separation, and 'absolute testing'. Ann CIRP 1996;45(2):617–34.
[10] Marsh ER, Arneson DA, Martin DL. A comparison of reversal and multiprobe error separation. Prec Eng 2010;34(1):85–91.
[11] Tanaka H, Tozawa K, Sato H. Application of a new straightness measurement method to large machine tools. Ann CIRP 1981;30(1):455–9.
[12] Kiyono S, Asakawa Y, Inamoto M, Kamada O. A differential laser autocollimation probe for on-machine measurement. Prec Eng 1993;15(2):68–76.
[13] Kiyono S, Gao W. Profile measurement of machined surface with a new differential method. Prec Eng 1994;16(3):212–8.
[14] Gao W, Kiyono S. Development of an optical probe for profile measurement of mirror surfaces. Opt Eng 1997;36(12):3360–6.
[15] Gao W, Kiyono S. New multiprobe method of roundness measurements. Prec Eng 1996;19(1):37–45.
[16] Elster C, Weingartner I. Exact wave-front reconstruction from two lateral shearing interfergrams. J Opt Soc Am A 1999;16(9):2281–5.
[17] Elster C, Weingartner I. Solution to the shearing problem. Appl Opt 1999;38(23):5024–31.
[18] Chen X, Kotani K, Takamasu K. Study on spatial frequency domain 2-point method (1st report): calibration of systematic error in case of combining two sets of 2-point method. J JSPE 2007;73(6):563–8.
[19] Fung EHK. An experimental five-sensor system for measuring straightness and yawing motion errors of a linear slide. Meas Sci Technol 2008;19:14, 075102.
[20] Fung EHK, Yang SM. An error separation technique for measuring straightness motion error of a linear slide. Meas Sci Technol 2000;11:1515–21.
[21] Liu SJ, Watanabe K, Chen X, Takahashi S, Takamasu K. Profile measurement of a wide-area resist surface using a multi-ball cantilever system. Prec Eng 2009;33:50–5.
[22] Yang P, Takamura T, Takahashi S, Takamasu K, Sato O, Osawa S, et al. Development of high-precision micro-coordinate measuring machine: multi-probe measurement system for measuring yaw and straightness motion error of XY linear stage. Prec Eng 2011;35:424–30.
[23] Yang P, Shibata S, Takahashi S, Takamasu K, Sato O, Osawa S, et al. A multi-probe measurement method to evaluate the yaw and straightness errors of XY stage on high precision CMM. Key Eng Mater 2010;447–448:590–4.
[24] Yang P, Shibata S, Takahashi S, Takamasu K, Sato O, Osawa S, et al.Development of high precision coordinate measuring machine (CMM) (1st report, evaluation method of XY stage). JSPE autumn conference; 2009. p. 725–6.

[25] Yang P, Shibata S, Takahashi S, Takamasu K, Sato O, Osawa S, et al.Development of high precision coordinate measuring machine (CMM) (2nd report, pre-experiment of multi-probe method for evaluating the XY stage). JSPE spring conference; 2010. p. 377–8.

[26] Takamura T, Yang P, Takahashi S, Takamasu K, Sato O, Osawa S, et al.Development of high precision coordinate measuring machine (CMM) (3rd report, evaluation of the form of referential mirror and the kinematic error of stage by 3-probe method). JSPE autumn conference; 2010. p. 515–6.